6362–6374 *Nucleic Acids Research, 2017, Vol. 45, No. 11* *Published online 3 April 2017*
doi: 10.1093/nar/gkx220

The elongation factor Spt4/5 regulates RNA polymerase II transcription through the nucleosome

John B. Crickard[1], Jaehyoun Lee[2], Tae-Hee Lee[2] and Joseph C. Reese[1,*]

[1]Department of Biochemistry and Molecular Biology, Center for Eukaryotic Gene Regulation, Penn State University, University Park, PA 16802, USA and [2]Department of Chemistry, Penn State University, University Park, PA 16802, USA

Received December 29, 2016; Revised March 21, 2017; Editorial Decision March 22, 2017; Accepted March 23, 2017

ABSTRACT

RNA polymerase II (RNAPII) passes through the nucleosome in a coordinated manner, generating several intermediate nucleosomal states as it breaks and then reforms histone–DNA contacts ahead of and behind it, respectively. Several studies have defined transcription-induced nucleosome intermediates using only RNA Polymerase. However, RNAPII is decorated with elongation factors as it transcribes the genome. One such factor, Spt4/5, becomes an integral component of the elongation complex, making direct contact with the 'jaws' of RNAPII and nucleic acids in the transcription scaffold. We have characterized the effect of incorporating Spt4/5 into the elongation complex on transcription through the 601R nucleosome. Spt4/5 suppressed RNAPII pausing at the major H3/H4-induced arrest point, resulting in downstream re-positioning of RNAPII further into the nucleosome. Using a novel single molecule FRET system, we found that Spt4/5 affected the kinetics of DNA re-wrapping and stabilized a nucleosomal intermediate with partially unwrapped DNA behind RNAPII. Comparison of nucleosomes of different sequence polarities suggest that the strength of the DNA–histone interactions behind RNAPII specifies the Spt4/5 requirement. We propose that Spt4/5 may be important to coordinate the mechanical movement of RNAPII through the nucleosome with co-transcriptional chromatin modifications during transcription, which is affected by the strength of histone–DNA interactions.

INTRODUCTION

Chromatin impedes RNAPII processivity across the body of a gene. The smallest repeating unit of chromatin is the nucleosome core particle, which wraps DNA ∼1.65 times around the histone octamer composed of one copy of the H3/H4 tetramer and two copies of the H2A/B dimer (1,2). Tight wrapping of the DNA on the octamer surface affects how efficiently RNAPII can progress through the nucleosome, and RNAPII is prone to arrest at major histone–DNA contact sites (3–9). The two most prominent arrest locations correspond to DNA contacts between the H2A/H2B dimer and H3/H4 tetramer, located ∼15–30 bp and 45–55 bp into the nucleosome, respectively (6–8). While these arrest points have been mapped or inferred from biochemical studies using artificial DNA sequences, high resolution nascent transcript sequencing studies in yeast confirm these arrest sites across the genome (10).The early (+15–30) and middle (+50) arrest sites have been attributed to defined intermediate states generated by the stepwise progression of RNAPII through the nucleosome. The early arrest site represents DNA uncoiled from the dimer surface with RNAPII undergoing backtracking along the DNA (5,11). The middle arrest site is generated when RNAPII reaches the H3/H4 interface and DNA is completely unwrapped from the nucleosome. RNAPII must wait for DNA to re-coil back onto the surface of the octamer, placing RNAPII in a stable loop or bulge of DNA removed from the surface of the nucleosome (7,12,13). The dynamic changes in the association of DNA with the octamer during transcription have been inferred by a number of assays (3–6,8,12); however, a high resolution, time-resolved direct measure of the uncoiling and recoiling of DNA has not achieved. Because DNA re-wrapping appears to be a rate limiting step in transcription through the nucleosome, this intermediate becomes a logical target for the function of transcription elongation factors (EFs) that facilitate RNAPII movement through the nucleosome.

EFs have evolved to facilitate the processivity of RNAPII across the body of genes. Several EFs known to affect RNAPII movement through the nucleosome include TFIIS, TFIIF, FACT and Paf1C (5,14–19). EFs can act directly on RNAPII, as in the case of TFIIS and TFIIF (16,20,21) or on the nucleosome, as with FACT (14,22,23). Early in the gene, the transcription processivity factor Spt4/5 is recruited to the elongation complex to become an integral structural component of the EC (24–27). Spt4/5 bridges the

*To whom correspondence should be addressed. Tel: +1 814 865 1976; Fax: +1 814 863 7024; Email: Jcr8@psu.edu

cleft of RNAPII, encircling the DNA, potentially placing Spt4/5 in competition with histone proteins for DNA and suggests that collision between the Spt4/5:RNAPII elongation complex and nucleosomes is likely. Furthermore, the ability of Spt4/5 to bind DNA exiting RNAPII could affect the re-wrapping of DNA back onto the octamer surface; thus, change the ability of RNAPII to navigate the nucleosomal barrier. Despite the probable physical confrontation between Spt4/5 and the nucleosome during transcription, the consequence of the collision between Spt4/5-containing ECs and the nucleosome is unknown. Here we characterize the effects of incorporating Spt4/5 into ECs on the progression of RNAPII through the nucleosome using both biochemical and single molecule FRET systems. Our study provides the first molecular glimpses into how the incorporation of EFs in the elongation complex affects RNAPII movement through the nucleosome and identifies a nucleosomal intermediate that may regulate co-transcriptional chromatin modifications.

MATERIALS AND METHODS

Generation of nucleosomal transcription templates

The 601 nucleosome positioning sequence (NPS) (28) was inserted into a transcription template containing a 70 nt G-less cassette, which was then used to prepare a transcription template bearing a 3′ overhang as described in previous publications (29–32). *Saccharomyces cerevisiae* histones were overexpressed in *Escherichia coli*, purified and then H2A and H2B and H3 and H4 were re-folded together to produce dimer and tetramer as previously described (1,33,34). H2A/B dimer and H3/H4 tetramer were purified on a Bio-rex 70 column (35) and used to assemble a nucleosome onto the transcription template using the histone chaperone Nap1 (33,34). Extent of reconstitution was monitored by EMSA on a 4% native page, and reconstitutions with <5% free DNA were used.

Purification of Spt4/5

Native Spt4/5 was purified from 12 l of *S. cerevisiae* containing tandem affinity tagged version of Spt4. Cells were re-suspended in 20 ml/l of culture in extraction buffer (200 mM Tris-acetate (pH 7.9), 390 mM ammonium sulfate, 10 mM $MgSO_4$, 1 mM ethylenediaminetetraacetic acid (EDTA), 2 mM dithiothreitol (DTT) and 20% glycerol supplemented with 1 mM phenylmethylsulfonyl fluoride (PMSF), 0.5 ug/ml leupeptin and 1 μg/ml pepstatin A. Cells were lysed by bead beating and the lysate was clarified by centrifugation at 10 000 × *g* for 30 min, followed by a spin at 40 000 rpm in an ultracentrifuge for 1.5 h. Solid ammonium sulfate was added to the supernatant with stirring until a final concentration of 65% was achieved. The proteins were collected by centrifugation at 10 000 × *g* for 30 min and the pellet was re-suspended in 20 ml of IgG binding buffer (40 mM HEPES pH 7.5, 200 mM NaCl, 0.1% Tween-20 and 10% glycerol containing the protease inhibitors listed above and dialyzed for 4 h against the same buffer with two buffer changes. IgG-sepharose (GE Life Sciences) was added and incubated overnight with rotation at 4°C. The beads were washed 2× with IgG binding buffer and 2× with Tobacco Etch Virus (TEV) protease cleavage buffer (10 mM Tris-Cl pH 8.0, 150 mM NaCl, 0.1% NP-40, 0.5 mM EDTA, 10% glycerol, 1 mM DTT, with 1 mM PMSF). Spt4/5 was liberated from the beads by digestion with 10 units of TEV protease overnight at 4°C. The flow through from the IgG beads was collected and the beads were washed with calmodulin binding buffer (10 mM Tris-Cl pH 8.0, 300 mM NaCl, 1 mM MgOAc, 2 mM $CaCl_2$, 0.01% NP-40, 10% glycerol, 0.5 mM DTT with the protease inhibitors listed above. The IgG wash and flow through were pooled, and incubated with calmodulin-sepharose beads for 4 h at 4°C. After two washes with calmodulin binding buffer, the protein was eluted with five column volumes of calmodulin elution buffer (10 mM Tris-pH 8.0, 150 mM NaCl. 1 mM MgOAc, 10 mM EGTA, 0.01% NP-40, 10% glycerol, 0.5 mM DTT. Peak fractions were pooled and passed over a 250 μl bed volume SP-Sepharose column. Spt4/5 was then eluted with a step gradient of 150, 250, 350, 800 and 1000 mM KCl in S-buffer (10 mM Hepes 7.5, X KCl, 6 mM $MgCl_2$, 1 mM DTT, 0.1% NP-40, 1 μM ZnCl2, 10% glycerol). Fractions containing Spt4/5 were then dialyzed against S-buffer with 150 mM KCl overnight at 4°C. Protein samples were flash frozen and stored at −80°C. Recombinant Spt4/5 was expressed in *E. Coli* and purified as described in a previous publication (27).

In vitro transcription on chromatin templates

RNAPII (∼200 fmol based on protein amount) was incubated with 40 ng DNA template for 10 min in 50 mM Hepes pH 7.5, 150 mM KCl, 1 mM $MnCl_2$, 0.5 mM DTT, 10% glycerol, 0.01 mM UpG, 0.1 μg/μl bovine serum albumin (BSA) and 1 unit/μl RNAsin. Transcription was initiated by adding a nucleotide mix containing 0.1 mM adenosine triphosphate (ATP), 0.1 mM CTP, 0.001 mM UTP and 0.0015 μM ^{32}P-alpha-UTP (6000 ci/mmol). After a 5 min pulse to produce radiolabeled RNA up to the G-tract, runoff was initiated by adding 0.1 mM ATP, 0.1 mM CTP, 0.1 mM UTP and 0.1 mM GTP. Reactions were terminated with 2× the volume of stop buffer (30 mM Tris–Cl pH 8.0, 5 mM EDTA, 100 mM NaCl, 1% sodium dodecyl sulphate) and then treated with 500 ng of Proteinase K for 20 min. Samples were then extracted with PCIAA (Phenol:Chlorform:Isoamyl Alcohol 1:0.9:0.01) and precipitated with ethanol in the presence of 4 μg of glycogen. RNA was resolved on 8% denaturing polyacrylamide gel electrophoresis, dried and exposed to a phophorimager screen. Images were captured on the Typhoon instrument (GE Biosciences) and processed by the ImageJ software.

RNAPII immobilization for exonucleaseIII mapping

Fifteen microliters of Protein A-sepharose magnetic beads (GE healthcare) blocked with 20 mM HEPES-NaOH pH 7.8, 150 mM NaCl, 10% glycerol, 250 ng/μl BSA was incubated with 1.5 μl of 8WG16 ascites fluid (Biolegend) for 1 h at room temperature. Beads were then washed 3× with 10 volumes of bead washing buffer (50 mM Tris-HCl pH 7.4, 250 mM KCl and 100 ng/μl BSA) and then 3× with IgG wash buffer (50 mM Tris-HCl pH 7.4, 100 mM NaCl). Approximately 4 pmol of RNAPII was then immobilized

on the beads in transcription buffer for 1 h at 4°C, washed 3× with IgG wash buffer, and resuspended in 40 μl transcription buffer. A total of 165 ng of 5′ ^{32}P-end-labeled templates was added and ECs were assembled for 20 min in presence of 100 μM CTP, ATP and UTP. Beads were then washed 3× with IgG wash buffer and 2× with 20 mM Hepes pH 7.5, 50 mM KCl, 5 mM $MgCl_2$, 1 μM $ZnCl_2$, 10% glycerol and 100 ng/μl BSA. Nucleotides, except for GTP, were added back to a final concentration of 100 μM and TFIIS was added in approximately equal molar concentration to RNAPII where indicated. EC nucleosome/DNA complexes were then eluted from the beads for 30 min at room temperature using recombinant 1.5 μg of glutathione-S-transferase (GST)-CTD. Elongation complexes were then chased for 5 min at 30°C by adding with 100 μM GTP. Samples were treated for 5 min with 10 units/μl ExonucleaseIII (NEB) and then terminated and the nucleic acids purified as analyzed as described above.

Single molecule FRET system

Fluorescent DNA templates were generated by annealing two complementary strands corresponding to the 601R sequence with Cy3 and Cy5 incorporated into the non-template strand at the +34 and +112 positions, respectively. The annealed DNA was then treated with T4 DNA ligase overnight and gel purified. The template strand had a small 4 bp overhang and was phosphorylated on the 5′ end. This extension was used to functionalize the template for transcription by ligation of a 42 bp double strand piece of DNA that contained a 13 bp 3′ single strand extension, which matched the template used in biochemical studies. The transcription templates were gel purified and nucleosomes were reconstituted as described above.

Quartz microscope slides were passivized by sequential sonication in acetone, dichloromethane and methanol for 15 min each. Followed by rinsing in deionized water and heating with a propane torch. Slides were washed in piranha solution (4 parts of 98% H_2SO_4 mixed with 1 part of 30% H_2O_2) for 1 h, rinsed thoroughly with deionized water and dried under a stream of nitrogen. A mixture of 99:1 of PEG-Silane (mPEG-Silane Mw 5000) from Laysan Bio, Arab AL and Biotin-PEG-silane (Biotin-PEG-Silane Mw 3400) was dissolved in anhydrous acetonitrile (Spectrophotometric grade, low water, OmniSolv, product No. AX0151-1) to a concentration of 100 μM by sonication. The polyethyleneglycol (PEG) reagents were obtained from Laysan Bio, Arab AL. The cleaned quartz slide was immersed in the PEG solution for 30 min with sonication, followed by additional sonication in acetonitrile twice for 5 min each to remove any residual unreacted PEG. The slide was sonicated again twice for 5 min each in deionized water and dried under nitrogen.

Streptavidin was flowed into the sample chamber at 0.1 mg/ml and then rinsed with Buffer A [10 mM Tris pH 7.8, 10 mM NaCl]. A total of 0.1 mg/ml of Biotin-protein A was flowed in and inucbated for 15 min, and then washed with buffer A. Purified 8WG16 IgG (0.1 mg/ml) was incubated with the slide for 2 h, followed by a wash. *In vitro* transcription reactions were formed in solution under the same conditions described above except with the addition of 4 mM PCA(protocatechuic acid), 0.4 μ/ml PCD(protocatechuate dioxygenase), 1 mM Trolox for imaging. Reactions were then injected into the sample chamber, and washed with transcription buffer. A complete mixture of NTPs and TFIIS (30 nM) were then injected and FRET signals monitored. TFIIS was added to rescue the significant fraction of ECs that became backtracked during immobilization.

smFRET data collection and analysis

Data were collected for fluorescence signals with a 532 nm laser illumination from individual nucleosome templates at a 250 ms time resolution for 20 min. The image of a slide surface containing nucleosome templates was spectrally divided into two regions (Cy3 and Cy5), aligned and projected to two separate regions on an EMCCD camera (Cascade II 512, Photometrics, Tucson, AZ). Fluorescence intensities from a Forster resonance energy transfer (FRET) donor and an acceptor at each time point were obtained by integrating the brightness of the corresponding pixels on the image. These intensities were utilized to calculate the apparent FRET efficiency from individual templates with the equation $I_A/(I_D + I_A)$, where I_D and I_A are the intensities of FRET donor and acceptor respectively. Within the 20 min of data collection time, 4 consecutive stacks of images were obtained from 4 different regions, with each stack containing data for 5 min from one region. At the end of each 5 min data collection period, we illuminated the sample surface with a 635 nm laser in order to test if an extinguished FRET acceptor is due to completely unwrapped DNA or due to photobleaching.

Time traces were analyzed with a three-state two-Gaussian mixture hidden Markov model as previously published (36).In the model, each FRET state is made of two separate states (i.e. two Gaussian mixture) in order to accommodate various FRET states due to multiple pause sites in the nucleosome. No analytical method is currently available to calculate the errors in a multi-parameter optimization. We used the data from numerical simulations as previously published (36) to estimate the errors in the hidden Markov model (HMM) results. In the simulations used in that paper, 318 events, which is smaller than what we analyzed here as evident from the FRET transition histograms (Figure 5B), result in 11.5% maximum average error (standard deviation). At a rate of 0.5 /s, which is faster than what we report here, a ΔFRET difference between 0.4 and 0.2 does not make a noticeable difference in the absolute amount of the error. We multiplied this maximum error 11.5% by 2 (= 23%) to widen the confidence interval to 95%. We are reporting this value, 23%, as our estimated error. Given the larger sizes of the datasets and the slower rates than those of the numerically simulated datasets (36), the 23% errors reported in Figure 5C should be likely the maximum errors at a 95% confidence level. This is a reasonable and only possible estimate that one can provide for HMM analyses. Upon visual inspection, we confirmed that nearly all of the transitions we can visually identify were detected in the HMM analysis. All of the FRET transitions identified by the analysis are shown as histograms in Figure 5B.

RESULTS

The arrest of RNAPII within the nucleosome is linker DNA-dependent

A nucleosome transcription template was designed by inserting the 601 NPS (28) downstream of a 70 bp G-less cassette (27,29–31,37). RNAPII initiates promoter-independent transcription from a single stranded 3′ extension using UpG dinucleotide (Figure 1A). Importantly, we have shown that ECs formed by this method are not prone to non-template strand displacement artifacts observed in other tailed-template systems (27,37). An RNA transcript is labeled with ^{32}P-UTP during the pulse phase, and then RNAPII stalls at a G-stop 20 bp ahead of the nucleosome. Transcription into the nucleosome is initiated by adding all four nucleotides and the progression of RNAPII through the nucleosome is monitored by transcript length. The template places the 'strong side' of the 601 NPS, as defined by single molecule studies (38), on the proximal side of the nucleosome facing RNAPII. This is the same configuration described as 601R in previous publications (8) and that used in atomic force single molecule experiments (3). It will be referred to as 601R from here on.

A nucleosome was assembled onto the template using recombinant yeast proteins, yNap1, yH2A/B dimer and yH3/H4 (Figure 1B) (33). We compared the transcription across the 601R NPS with and without a nucleosome (Figure 1C, free DNA (lanes 1–4) versus nucleosome (lanes 5–8)). As expected, assembling a nucleosome on the template led to reduced full length run off products and the appearance of nucleosome-specific arrests (Figure 1C). The predominant arrest points were observed early (+15–30 bp) and in the middle (∼+50 bp) of the nucleosome at moderate ionic strength (120 mM), which has been reported by others and correspond to contact points between the DNA and H2A/B and H3/H4, respectively (7,8,39). Enhanced RNAPII arrest was observed also prior to the entry point of DNA into the octamer. This may be attributable to histone tail–DNA interactions, which contribute to RNAPII arrest ahead of the nucleosome core particle (3,40).

Next, we compared RNAPII arrest within the nucleosome at different ionic strengths, 40-, 120- and 375 mM KCl. The binding of DNA to H2A/H2B is more sensitive to ionic strength than its binding to H3/H4, and we anticipated that arrests early in the nucleosome (+15–30) would be more sensitive to salt concentrations. As expected, RNAPII arrest points early in the nucleosome decreased and those in the middle regions accumulated as ionic strength increased (Figure 1C and Supplementary Figure S1). The early arrest points were mostly eliminated at 375 mM, an ionic strength that disrupts H2A/H2B dimer–DNA interactions. Arrests in the middle region of the nucleosome, corresponding to H3/H4 tetramer contact points (+50), were less sensitive to the salt concentrations used here. These results indicate that we accurately recapitulated RNAPII arrest with in the nucleosome that correlated with major histone–DNA contact points in the nucleosome.

Interestingly, an arrest point located past the dyad of the nucleosome (+90 from the entry point) increased with higher ionic strength and was prominent at 375 mM (Figure 1C and Supplementary Figure S1). This late arrest site was not observed (or was not prominent) in earlier biochemical studies using a transcription template with no extranucleosomal (linker) DNA downstream of the nucleosome (8). However, an arrest past the nucleosome dyad, which may correspond to the +90 site described here, had been inferred from single molecule force measurements using templates with linker DNA (3). We hypothesized that linker DNA downstream of the nucleosome, in the direction of transcription, may influence the locations of RNAPII arrest. This was tested by mapping RNAPII arrest points on templates containing either 0 or 45 bp of extranucleosomal DNA downstream of the 601R positioning sequence. The template with 45 bp of linker DNA (N45) produced RNAPII arrest at the +90 site at lower ionic strength compared to the template lacking linker DNA (Figure 2A, lanes 6–7 versus lanes 2–3 and Supplementary Figure S2). Furthermore, a greater proportion of RNAPII arrested at the middle arrest sites (+50) on the N45 template at lower ionic strength than on the version lacking linker DNA (N0). The differences in RNAPII arrest on templates with or without linker became negligible at higher ionic strength (Figure 2A, lane 4 versus lane 8 and Supplementary Figure S2), as the late arrests were observed even when no linker was present. To further confirm this observation, we constructed templates with varying lengths of DNA downstream of the 601R nucleosome, 45, 15 and 0 bp, and compared the arrest of RNAPII on these templates at a moderate (120 mM) ionic strength. We observed that as linker length increased, RNAPII arrested at locations deeper within the nucleosome. A total of 15 bp of linker DNA was required for strong formation of the arrest sites near the dyad axis, and 45 bp of linker was required for the formation of the +90 arrest (Figure 2B and Supplementary Figure S3). From this we conclude that downstream extranucleosomal DNA is a regulator of RNAPII progression through the nucleosome, and has a similar effect as breaking histone DNA contacts using ionic strength. The linker-length dependence observed here may be explained by the enhanced 'breathing' of DNA off the surface of the octamer on nucleosomes containing linker DNA (41). Thus, collectively, the data suggest that the formation of the late arrest point is dependent on the dynamics or strength of DNA–octamer interactions, which can be achieved by adding linker or increasing ionic strength.

Formation of late arrest points does not involve nucleosome re-positioning

A previous study indicated that RNAPII transcribes through the nucleosome without changing the translational position of the nucleosome along the DNA (12). However, it is possible that the linker-dependent formation of the late arrest sites is caused by transcription-dependent re-positioning or sliding of the nucleosome downstream. In order to test this possibility, we used exonucleaseIII (exoIII) to map the edge of the nucleosome. Transcription induced re-positioning of the histone octamer would result in novel exoIII stops along the DNA downstream of the nucleosome. Since most templates in transcription reactions are not utilized by RNAPII, templates engaged in transcription

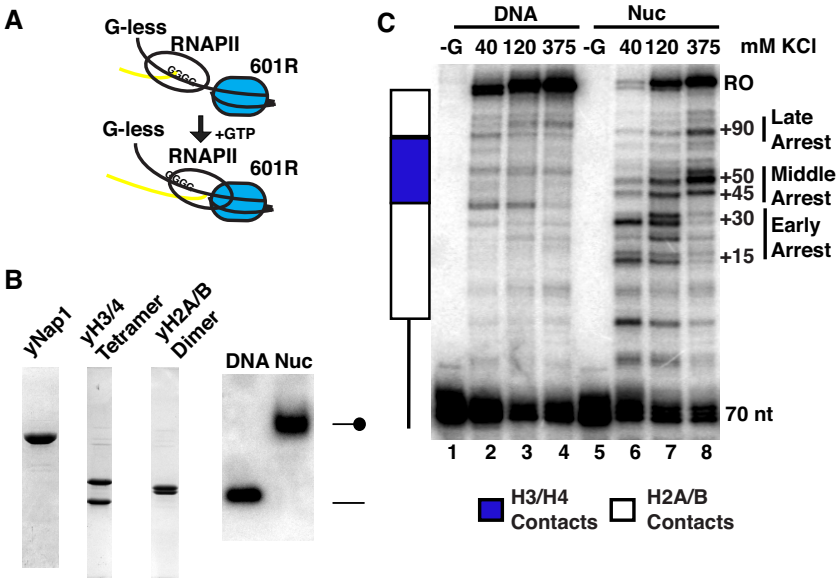

Figure 1. RNAPII nucleosome transcription system. (**A**) Schematic representation of the transcription template, which contains a 70 bp G-less cassette, followed by a G-tract and the 601R nucleosome positioning sequence (NPS) located downstream. The G-tract is located 20 bp from the nucleosome entry site. (**B**) Sodium dodecyl sulphate-polyacrylamide gel electrophoresis (SDS-PAGE) of components used to assemble yeast nucleosomes and EMSA of a typical nucleosome reconstitution. (**C**) *In vitro* transcription on free DNA (lanes 1–4) and nucleosomal templates (lanes 5–8). ECs (EC70) were formed in low salt in the absence of GTP and then salt was added to the concentrations listed above the panel. The samples in the lanes 1 and 5 labeled '-G' were not chased with GTP. Run-off was conducted for 10 min after the addition of a complete nucleotide mix. A schematic representation of the nucleosome is shown on the left. H2A/B dimer and H3/H4 tetramer contact points are shown in white and gray, respectively.

were enriched by immobilizing RNAPII on beads using an antibody to the C-terminal domain (CTD) of Rbp1 (Figure 2C). ECs were formed on beads, unutilized templates washed away and the ECs were eluted from the beads using recombinant GST-CTD as previously described (27). ExoIII footprinting was then performed after RNAPII ran into the nucleosome (+GTP) or remained stalled at the G-tract ahead of the nucleosome (−GTP). The major exoIII stop was detected 45 bp from the end of the template, at the downstream edge of the nucleosome (Figure 2D). Less intense nucleosome-induced stops displaying ∼10 bp periodicity were detected further into the nucleosome, caused by exoIII pausing at the major DNA–histone contacts on the surface of octamer as others have observed (42). The same major exoIII stop (45 bp) was observed on free nucleosomal templates not undergoing transcription, indicating that transcription on the template upstream of the nucleosome during the 'pulse' phase, or the immobilization process did not alter nucleosome positioning (Supplementary Figure S4). Importantly, the position of the exoIII stops did not change when GTP was added and RNAPII ran into the nucleosome (Figure 2D, compare lanes 1 and 2), indicating that transcription did not re-positioning the octamer downstream along the DNA. Thus, the increase in the late arrest site in the presence of linker DNA is not caused by the sliding of the nucleosome into a downstream position and is consistent with RNAPII transcribing deeper into the nucleosome.

Spt4/5 affects RNAPII progression into the nucleosome

The progression of RNAPII through the nucleosome is dependent upon cycles of DNA unwrapping ahead of RNAPII and re-wrapping behind it (4,5,7,8). EF associated with RNAPII have the potential to influence histone–DNA contacts during transcription, especially factors that have the capacity to bind to DNA in the EC. One such factor is Spt4/5, which is an integral part of the EC and contacts the non-template strand in the transcription bubble and DNA exiting RNAPII (24,25,27). Native Spt4/5 was purified from yeast using tandem affinity purification (TAP), followed by ion-exchange chromatography (Figure 3A). Transcription of the 601R template containing 45 bp of linker DNA downstream of the nucleosome was performed in the absence and presence of Spt4/5. Adding Spt4/5 did not result in a large increase in full-length run off products, but instead altered the location of RNAPII arrest within the nucleosome (Figure 3B). Strikingly, Spt4/5 suppressed the middle arrest sites (+50 bp) at the major DNA-H3/H4 contact points in the nucleosome and increased the accumulation of a late arrest site located at +90 (Figure 3B, lanes 3–5 versus 6–8 and Supplementary Figure S5). The Spt4/5 affect is nucleosome specific, because Spt4/5 did not alter RNAPII transcription on naked DNA (Supplementary Figure S5). The shift in RNAPII arrest was quantified by calculating the ratio of the signal at the late versus middle arrest, which revealed that Spt4/5 caused a reproducible 2–3-fold increase in the +90/+50 ratio (Figure 3C). Interestingly, Spt4/5 had no effect on the early arrest sites (15–30 bp), suggesting that its ability to suppress pausing (27) is not fully responsible for its effects on transcription through a nucleosome and that Spt4/5 acts on a specific intermediate formed during transcription. The shift in arrest sites was also observed when recombinant Spt4/5 produced in *E. coli* was used (27); thus, the activity described here is not

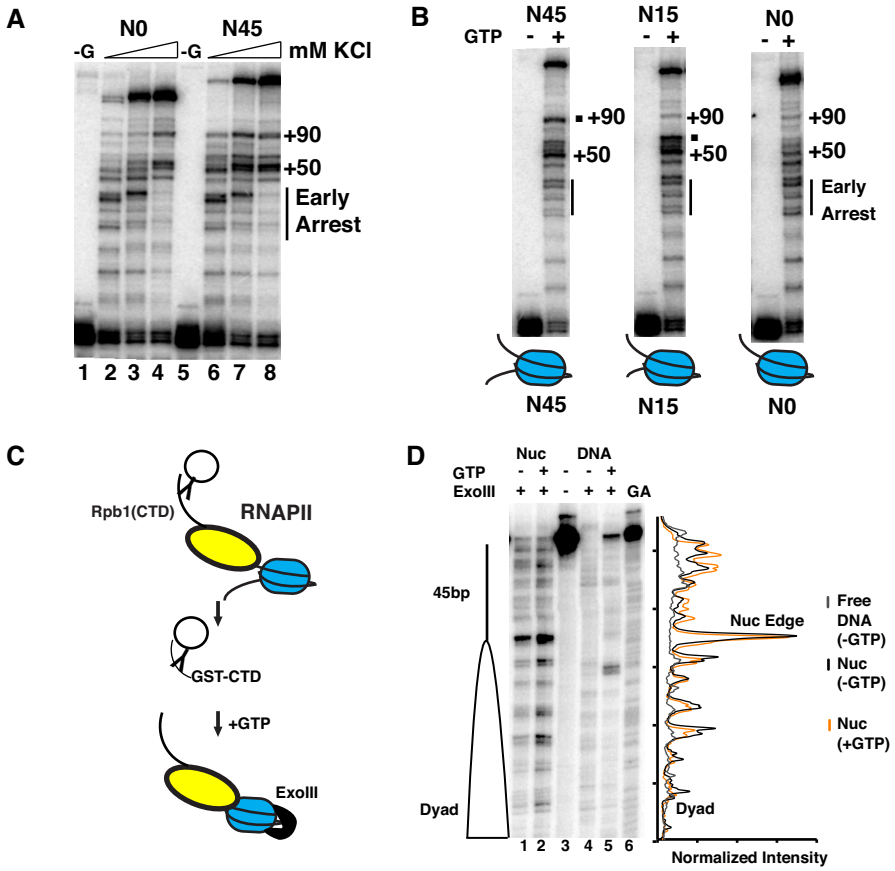

Figure 2. Downstream extranucleosomal DNA regulates RNAPII arrest. (**A**) Transcription of nucleosomes without (lanes 1–4, N0) and with 45 bp of extranucleosomal DNA downstream (lanes 5–8, N45). Run-off was carried out at different salt concentrations as described in Figure 1. (**B**) Transcription of nucleosome templates containing 45-, 15- and 0 bp of downstream extranucleosomal DNA. Transcription was carried out at 120 mM KCl. Dots label arrests sites enriched on templates containing 15 and 45 bp linker DNA. Lanes were cropped from the same gel, but only the most relevant lanes are shown. Scans of the gels can be found in Supplementary Figures S2 and 3. (**C**) Schematic drawing of the solid-phase transcription system used in exonuclease III mapping. (**D**) Exonuclease III mapping of the downstream edge of the nucleosome. Assays were carried out on the N45 template when RNAPII was chased into the nucleosome (+GTP, lane 2) or when arrested before the nucleosome (−GTP, lane 1). Transcription on free DNA was also analyzed (lanes 4 and 5). The stops observed in the naked DNA lanes in reactions with GTP likely results from arrested RNAPII. A GA marker is located in lane 6 and used to identify the locations of the exoIII-generated footprints. A normalized trace of lanes 1 (black), 2 (orange) and 4 (blue) is shown to the right and was produced using Image Quant software. The gel was cropped to show the region close the edge of the nucleosome.

due to contaminants in the source purified Spt4/5 (Supplementary Figure S6A and B). Additionally, a mutant version of Spt4/5, Spt4/5 (1–418), that cannot stably bind RNAPII (27) was unable to function in this assay (Supplementary Figure S6 C and D), indicating that Spt4/5 must be incorporated into the EC to affect transcription through the nucleosome. The C-terminal region of Spt5 indirectly affects chromatin transcription by recruiting Paf1c and mediating co-transcriptional histone modifications (43–46); however, the nucleosome transcription promoting activity of Spt4/5 is not dependent upon the C-terminal repeat (CTR) of Spt5 (Supplementary Figure S6C and D). Thus, this is the first evidence that Spt4/5 directly affects RNAPII passage through a nucleosome, which is distinct from its ability to recruit chromatin modifying complexes through the CTR.

Spt4/5 activity requires extranucleosomal DNA downstream of the nucleosome

The results described above suggest that Spt4/5 acts on a specific nucleosome intermediate generated during transcription, rather than just generally reducing RNAPII pausing throughout the nucleosome. As described above, the RNAPII arrest intermediates can be changed by altering the length of linker DNA downstream of the nucleosome (Figure 2A and B). The late arrest point (+90) generated by Spt4/5 is the same arrest point that is sensitive to the length of linker DNA (Figure 2A and B), which prompted us to explore the relationship between the length of linker DNA and the action of Spt4/5 on transcription through the nucleosome.

The activity of Spt4/5 on nucleosomes with increasing lengths of linker DNA was examined. On templates containing 45 bp of linker DNA, Spt4/5 suppressed the major middle arrest point at +45/50 and shifted RNAPII to the later arrest point as described above (Figure 4A). How-

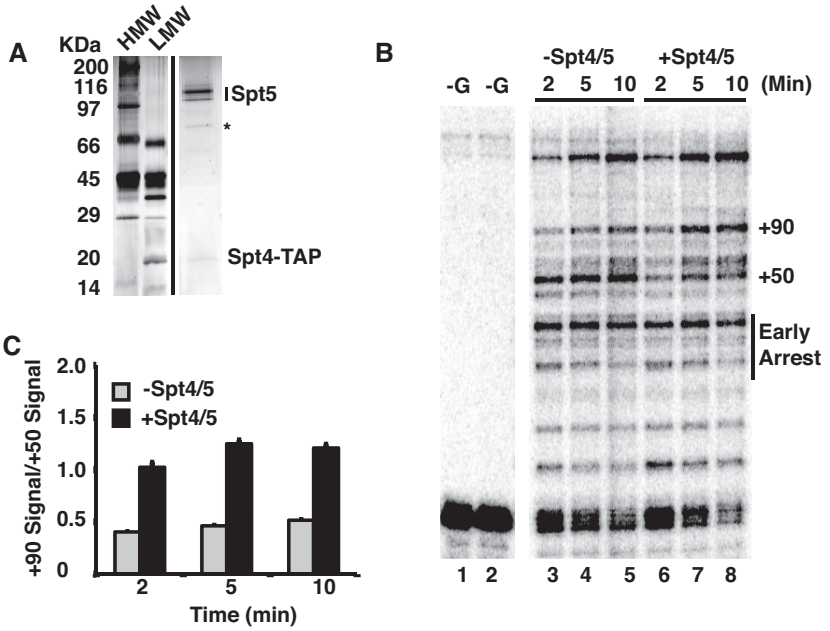

Figure 3. Spt4/5 promotes RNAPII progression into the nucleosome. (**A**) SDS-PAGE of Spt4/5 purified from yeast containing a TAP-tagged (52) version of Spt4. The gel was stained with silver. Spt5 migrates as multiple species attributable to its phosphorylation of the CTR (52). The asterisks marks a degradation product of Spt5. High- and low molecular weight markers (HMW, LMW) are indicated. The Spt4/5 sample was cropped to place it adjacent to the markers (**B**) Transcription of the 601R template was conducted in the absence (lanes 1, 3–5) or presence (lanes 2, 6–8) of Spt4/5. Three-fold molar excess of Spt4/5 relative to RNAPII was used, which is sufficient to bind all RNAPII ECs under the conditions used here (27). ECs were formed by transcription up to the G-tract, incubated with Spt4/5 and then chased for 2, 5 and 10 min by the addition of cold nucleotides, including GTP. The samples run without GTP (−G) were run on the same gel. Cropping is indicated by a space. A scan of the gel can be found in Supplementary Figure S5. (**C**) Quantification of ratio of the +90/+50 arrest sites. RNAPII alone (gray) and RNAPII+Spt4/5 (black). Values are the means and SEMs of three independent experiments.

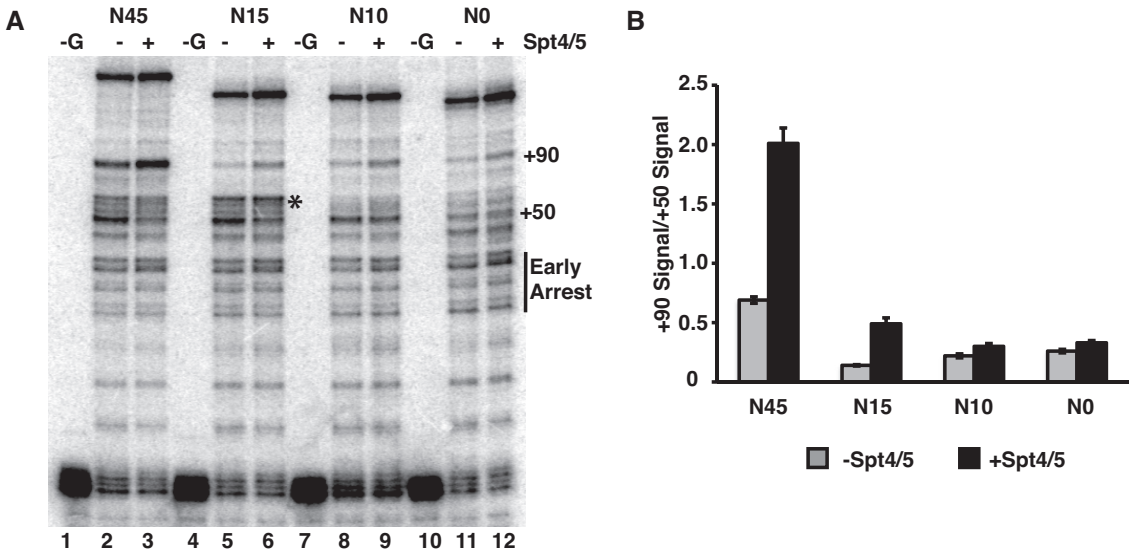

Figure 4. Spt4/5 activity requires downstream extranucleosomal DNA. (**A**) Transcription from nucleosome templates with 45, 15, 10 or 0 bp of downstream linker DNA. Three-fold excess of Spt4/5 compared to RNAPII was used where indicated. The lanes marked with −G were not chased with GTP. (**B**) Quantification of the +90/+50 ratio for each template. Black and gray bars are the values with or without Spt4/5 respectively. The error bars represent the SEM from three independent experiments.

ever, Spt4/5 had no effect on transcription through nucleosomes with 10 bp or no linker DNA. Quantifying the ratio of the +90/+50 arrest sites revealed that the effectiveness of Spt4/5 to stimulate the penetration of RNAPII into the nucleosome decreased as a function of linker DNA length (Figure 4B). While shortening the linker to 15 bp reduced the Spt4/5-dependent appearance of the late arrest point at +90, Spt4/5 reduced arrest at +45/50 and enhanced a site close to the nucleosome dyad (Figure 4A, asterisk). Thus, the activity of Spt4/5 is linker DNA dependent and likely related to the formation and resolution of specific intermediates formed during transcription.

SmFRET analysis of RNAPII transcription through the nucleosome indicates that Spt4/5 affects DNA re-wrapping

Ensemble biochemistry assays suggest that DNA uncoiling and recoiling is essential for the progression of RNAPII through the nucleosome (7,11,12,14). We next established a single molecule FRET (smFRET) system to monitor the dynamics of DNA unwrapping and re-wrapping in real time during the transcription process to gain a mechanistic understanding of how Spt4/5 affects RNAPII movement through the nucleosome and the intermediates formed during transcription. To do so, acceptor and donor dye pairs were incorporated into the non-template strand at +34 (Cy5) and +112 (Cy3), which places the pair across from each other on the opposite gyres of DNA wrapped onto the nucleosome. Changes in FRET intensities measure the unwrapping and re-wrapping of DNA on the octamer as RNAPII passes through the nucleosome. ECs arrested at the G-stop were formed in solution and then immobilized on a microscope slide pre-coated with PEG and streptavidin using biotinylated protein-A conjugated to an antibody that binds the CTD of Rpb1, 8WG16 (Figure 5A, upper). Transcription through the nucleosome was initiated by injecting a solution containing all NTPs and TFIIS. FRET signals were recorded from individual nucleosomes for up to 20 min. TFIIS was added to rescue RNAPII that becomes backtracked during the immobilization procedure. No change in FRET intensity was observed on the vast majority (>99%) of the nucleosomes throughout the 20 min time frame when NTPs were omitted, verifying that the changes in FRET signals are dependent on transcription and not caused by spontaneous nucleosome disassembly.

The time traces of the FRET efficiencies were obtained from individual ECs after the release of RNAPII into the nucleosome. A representative trace is displayed in the lower panel of Figure 5A, which shows transitions between multiple FRET states. Three groups of FRET states were defined: high FRET (FRET efficiency >0.6) corresponding to a completely wrapped DNA on the octamer, mid FRET (FRET efficiency 0.3–0.6) indicating a partially unwrapped nucleosome and low FRET (FRET efficiency <0.3) indicating an unwrapped nucleosome state. A summary of sample smFRET traces for each transition is displayed in Supplementary Figure S7.

Data from multiple measurements were used to extract rate constants for transitions between two states (for example from high FRET to mid FRET or mid FRET to low FRET) using a three-state, two-Gaussian HMM (36) (Figure 5B and C; Supplementary Figure S8A and B). We excluded long-lived FRET states immediately before FRET acceptor photobleaching from the analysis because their durations cannot be measured properly. This filtering also ensures that we do not include permanent arrests in data analysis. A 2D histogram analysis of the major FRET transitions observed identified four different transitions (Figure 5B, left panel). There is a high to mid transition (H→M), mid to low (M→L), low to mid (L→M) and mid to high (M→H). Shown above the table is an illustration of hypothetical RNAPII positions within the nucleosome during each of the FRET states, assuming that the majority of the RNAPII molecules are progressing forward through the nucleosome (Figure 5C). It should be noted that the states with partially (mid FRET) or fully unwrapped (low FRET) DNA cannot be attributed definitely to a specific pause site because the states are convolved with multiple sub-states within a range of pause sites. However, the calculated lifetime pauses at each state correlate with the accumulation of RNAPII arrest sites at the major histone contacts with the DNA (Figure 1C and Figure 5C) and the biochemical observations of others (3,5,7,8,12). From this data we propose that the first mid-FRET state following the initial high FRET represents RNAPII entering the nucleosome and partially unwrapping DNA away from the surface of the octamer, followed by a low FRET state, attributable to the unwrapping of DNA caused by the deeper penetration of RNAPII into the nucleosome. The low FRET state represents a kinetically stable intermediate and likely captures the rate-limiting step in transcription through the nucleosome, presumably the +50 arrest point detected in the transcription assays, as previously suggested by other studies (Figure 5C) (3,7). We also observed that the mid FRET states can be further divided into one that occurs prior to unwrapping (mid-FRET 1) and another that occurs afterward and represents the partial re-wrapping of DNA back onto the octamer (mid-FRET 2). There is a significant difference in the average state lifetime depending on the preceding state, high to mid (9.1 s) or low to mid (3.8 s), which suggests after RNAPII clears the rate-limiting step it can go forward relatively unimpeded (Figure 5C).

Adding Spt4/5 brought about changes in the resident time of specific states during nucleosomal transcription. First, Spt4/5 significantly shortened the average lifetime of the low FRET state, suggesting it promotes RNAPII escape from the major nucleosomal barrier (Figure 5C). Second, while Spt4/5 had limited effect on the lifetime of the first mid-FRET state, it significantly increased the lifetime of the second mid FRET state (Figure 5C), suggesting the accumulation of a partially wrapped state after RNAPII cleared the major barrier. The stabilization of the partially unwrapped state is evident in 2D plots; the final M→H transition event is less abundant in the presence of Spt4/5 (Figure 5B, compare the areas on the left and right), indicating a decreased rate of DNA re-wrapping in the presence of Spt4/5. Comparing the Spt4/5-induced changes in lifetime pauses in the smFRET assays to the accumulation in arrest products allowed us to correlate the different FRET states depicted in Figure 5C to RNAPII arrest locations. Spt4/5 had no effect on the arrest intermediates early in the nucleosome (Figure 3), and consistently, it had no effect on the

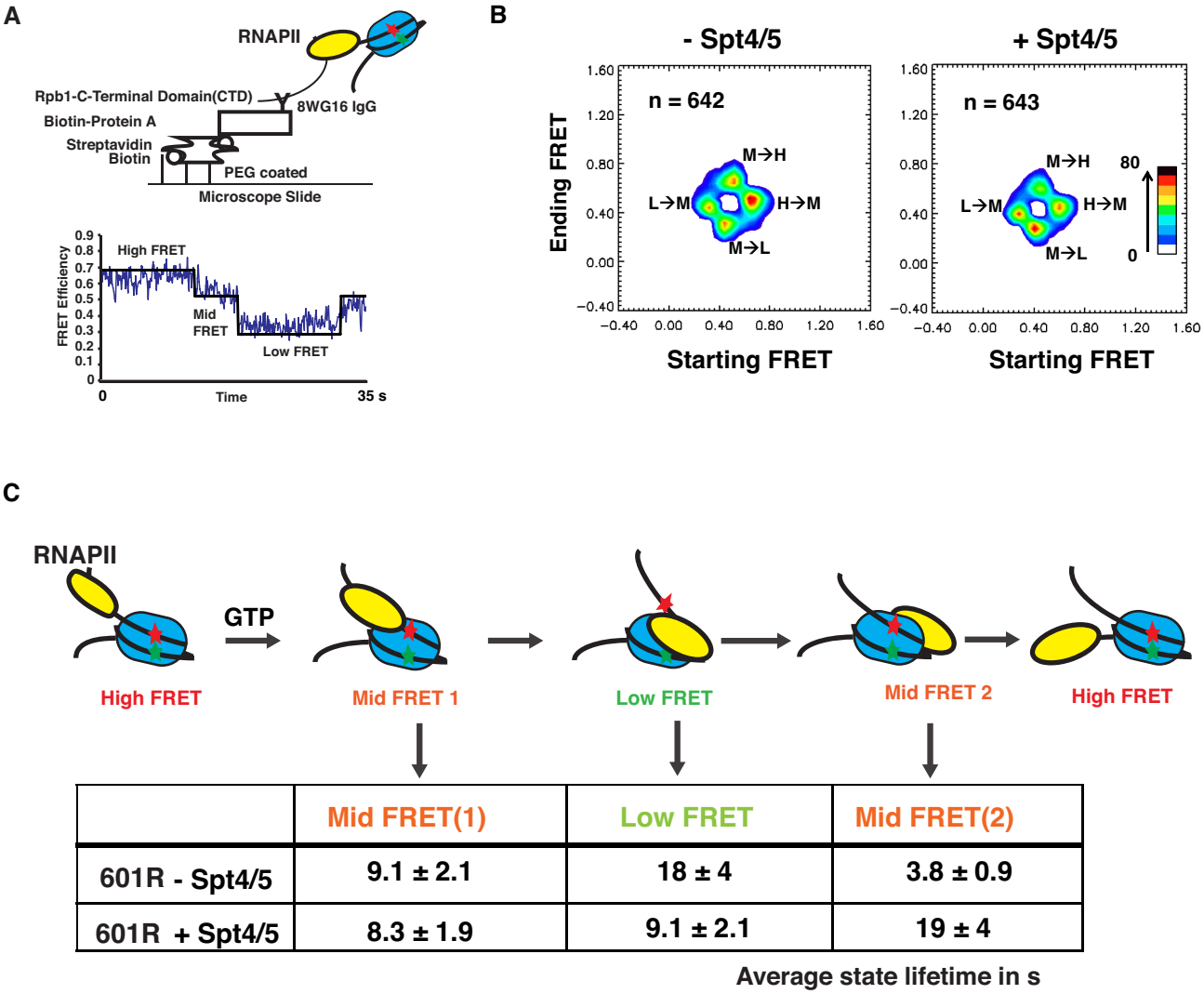

Figure 5. smFRET analysis of Spt4/5 effect on transcription through chromatin. (**A**, upper) Schematic for strategy to immobilize the RNAPII–nucleosome complex on microscope slides for smFRET analysis. (A, lower) A representative trace the FRET efficiencies between the fluorescent dyes. Congruent changes in both the Cy5 and Cy3 channels were required for the changes to be included in analysis. Efficiency levels were used to determine the state of the nucleosome structure. The time scale is 0–35 s. Additional sample traces showing each transition are given in Supplementary Figure S7. (**B**) The 2D histograms represent FRET transition counts from a starting FRET value (x-axis) to an ending FRET value (y-axis). The color code starts from white (0) to black (80) as shown in the color bar. The transition time points in a FRET time trace were identified by HMM analysis: 0.04 bins the starting and ending FRET values of a transition, and the histogram counts are smoothed using a boxcar average of 2 bins. The number of elongation templates analyzed is shown in the panel. (**C**) Schematic diagram of the hypothetical positions of RNAPII corresponding to each of the three FRET states (above). The table shows the average lifetime of each intermediate FRET state in seconds. The lifetimes are the reciprocals of the relevant kinetic rate constants obtained from the HMM analysis (Supplementary Figure S8).

pause time in mid-FRET 1 state (Figure 5C). In contrast, Spt4/5 greatly shortened the time in the low FRET state, which corresponded to reduced accumulation of +50 arrest product in biochemical assays. This followed a Spt4/5-dependent increase in mid-FRET 2 duration and the accumulation of the +90 arrest product. Our conclusions from these data is that Spt4/5 helps RNAPII escape a kinetically stable intermediate corresponding to the major nucleosomal barrier, while stabilizing a partially un-wrapped state of the nucleosome.

The inherent flexibility of the proximal DNA in the nucleosome affects Spt4/5 activity

The unwrapping of the 601 nucleosome under force occurs asymmetrically, where one half of the 601 nucleosome unravels first, followed by the other half of sequence (38). The 'strong side' contains the 10 bp TA steps at four turns of the DNA, which increases the flexibility of the DNA and the strength of DNA-octamer association (47). The 601R orientation used here positions the strong side half proximal to approaching RNAPII (Figure 6A). Previous studies have shown that the orientation of the 601 NPS relative to transcription determines the location and the strength

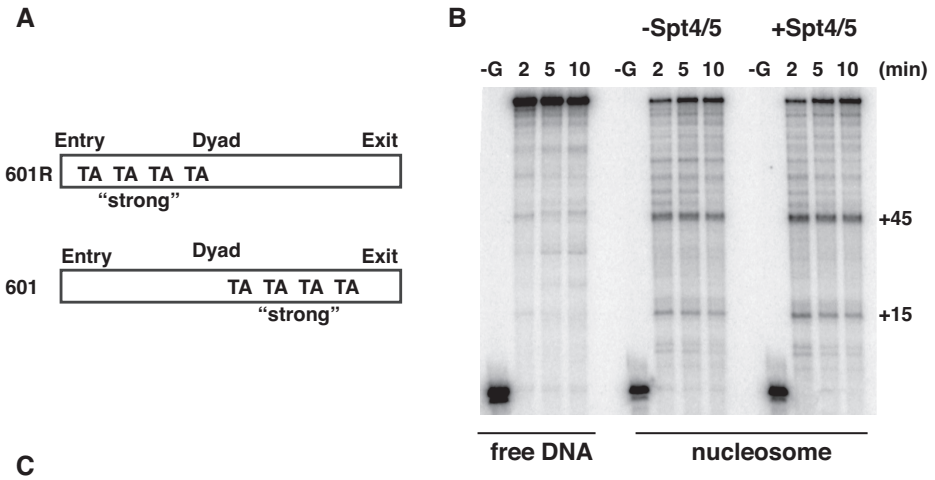

C

	Mid FRET(1)	Low FRET	Mid FRET(2)
601 - Spt4/5	9.1 ± 2.1	13 ± 3	14 ± 3
601 + Spt4/5	9.1 ± 4.0	9.1 ± 4.0	8.3 ± 3.7

Average state lifetime in s

Figure 6. Analysis of Spt4/5 on the 601 NPS. (**A**) Schematic representation of 601 NPS relative to the direction of transcription. The polarity of the sequence is indicated by the position of four consecutive TA dinucleotide steps on the face of the octamer relative to the dyad. The side with the four TA steps is the 'strong' side (see text). (**B**) *Invitro* transcription reactions comparing free DNA, nucleosomes and nucleosomes +Spt4/5 at 2-,5- and 10 min. (**C**) The table lists the average lifetime of each FRET state in the absence ($N = 658$) and presence of Spt4/5 ($N = 125$).

of RNAPII arrest, and the 601R orientation provides a stronger proximal barrier to transcription (8). Furthermore, biochemical analysis have shown that RNAPII forms different arrest intermediates on nucleosomes with the 601 versus the 601R orientation, including the point of arrest and the extent of re-wrapping of DNA behind RNAPII (11). We hypothesize that Spt4/5 may control the re-wrapping of DNA behind RNAPII. If true, the polarity of the 601 sequence will have an effect on the activity of Spt4/5.

We examined the activity of Spt4/5 on the 601 nucleosome, where the weaker side is proximal to transcription. In the absence of Spt4/5, fewer intense early arrests were observed on the 601 sequence and the major mid-arrest was detected closer to the DNA entry point in the nucleosome, at approximately +40–45 (Figure 6B, for comparison to 601R see Supplementary Figure S5A). This is in good agreement with previous reports (8). Unlike what was observed on the 601R nucleosome, Spt4/5 had little to no effect on RNAPII arrest patterns on the 601 sequence (Figure 6B and Supplementary Figure S9A). Next we analyzed RNAPII movement through the nucleosome using the smFRET system. Similar to the 601R sequence, 2D histogram analysis identified four major transitions (Supplementary Figure S9B). However, consistent with the ensemble biochemistry result, Spt4/5 did not change significantly the pause duration of any of the FRET states (Figure 6C and Supplementary Figure S9A). The lack of Spt4/5 effect on RNAPII pausing in the 601 sequence suggests that the flexibility of the DNA and the strength of the DNA–octamer interactions behind RNAPII determines the outcome of incorporating Spt4/5 into the EC during nucleosomal transcription.

DISCUSSION

The mechanism of how RNAPII navigates the nucleosomal barrier has been studied extensively using pure RNAPII, but how the incorporation of EFs into the EC affects this process is poorly understood. This study advances our understanding of this process by defining how Spt4/5, an integral part of the EC, affects transcription through the nucleosome. We report for the first time that Spt4/5 directly affects how RNAPII transcribes through a model nucleosome, an activity that is distinct from its recruitment of the Paf1c and associated chromatin remodeling factors. Using a combination of biochemical and single molecule FRET analyses we showed that Spt4/5 suppresses arrest of RNAPII at a specific intermediate located +50 bp into the 601R nucleosome by reducing the lifetime of an unwrapped state during transcription. We show that suppression of the +50 arrest results in relocation of RNAPII to a site roughly 90 bp into the nucleosome, and the stabilization of a partially unwrapped nucleosome structure. Furthermore, we show that the strength of the DNA–histone interactions behind RNAPII and the nucleosomal intermediates generated by different DNA sequences affects how Spt4/5 impacts nucleosomal transcription. We discuss this difference in the context of previous studies on the properties of the polarity of the 601 sequence and the unique structural intermediates generated during RNAPII transcription.

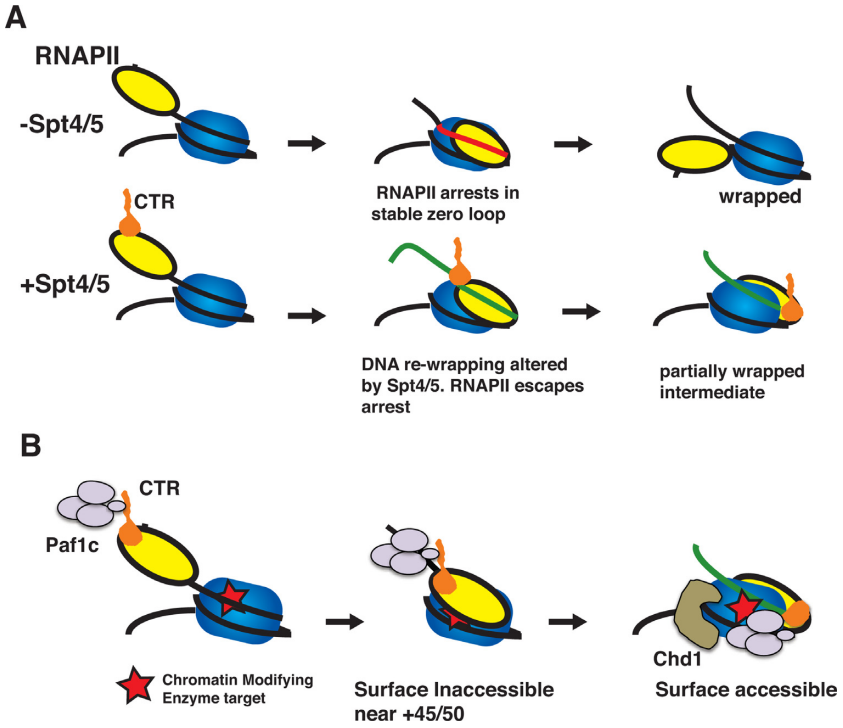

Figure 7. Spt4/5 coordinates the mechanical movement of RNAPII through the nucleosomes with co-transcriptional modification of chromatin. (**A**) Contact between Spt4/5 and DNA affects the re-wrapping of DNA back onto the nucleosome behind RNAPII, allowing RNAPII to escape the +45/50 arrest site and repositioning itself downstream past the dyad. (**B**) The Spt4/5-induced movement of RNAPII and stabilization of the partially unwrapped nucleosome allows accessibility of surfaces on the octamer to histone modifying enzymes that are associated with the CTR of Spt5 during transcription.

Spt4/5 acts on nucleosomal intermediates

Spt4/5 prevents RNAPII pausing/arrest on naked DNA (27), and it is tempting to attribute all of its functions during nucleosomal transcription to this activity. However, a number of observations argue against a generic mechanism whereby Spt4/5 allows RNAPII to work its way through the nucleosome by simply suppressing pausing/arrest. RNAPII arrests at multiple positions in the nucleosome, but Spt4/5 acted on intermediate(s) formed on the 601R sequence at the major arrest point at the H3/H4 DNA contact points. If Spt4/5 was generally preventing pausing, the expectation is that it would suppress arrest throughout the nucleosome and this activity would be observed on all templates tested. In contrast to Spt4/5, the potent anti-arrest factor TFIIS did not produce the specific arrest intermediates induced by Spt4/5, but generally promoted RNAPII progression through the nucleosome (Supplementary Figure S10A and B) (5,16). Furthermore, an Spt4/5 mutant with reduced anti-pausing activity on naked DNA (27) was able to promote RNAPII transcription through the nucleosome similar to wild-type Spt4/5 (Supplementary Figure S10C). Collectively these points argue that suppression of the +50 site on the 601R sequence is not due to a generic ability of Spt4/5 to prevent RNAPII pausing/arrest, but is attributable to a novel nucleosome-specific function of Spt4/5. The linker DNA dependence observed for Spt4/5 chromatin specific function is likely related to further progression of RNAPII into the nucleosome, resulting in intermediates that are affected by Spt4/5. Since the late arrest intermediate (+90) can be recapitulated in the absence of Spt4/5 under conditions that reduces histone DNA interactions (salt, linker DNA), this suggests Spt4/5 acts on or exploits intermediates generated by RNAPII, rather than actively generating these states and may do so by affecting the wrapping of DNA onto the surface of the octamer.

Differences in polarity suggest a role for Spt4/5 in controlling the re-wrapping of DNA back onto the octamer

Biochemical studies revealed that the orientation of the 601 sequence, relative to approaching RNAPII, has a profound effect on the RNAPII-generated nucleosomal intermediates (7,11,13). DNA wraps back onto the surface of the 601R nucleosome, forming a stable (zero-loop), trapping RNA polymerase at the major arrest point after transcribing 50 bases into the nucleosome (+50 described here and elsewhere) (7,11,13). On the other hand, RNAPII transcribing through the opposite orientation, the DNA remains 'peeled' off the surface behind RNAPII, as indicated by increased accessibility to nucleases and other measurements (11). This difference in re-wrapping on the two sequences may be explained by the flexibility of the DNA behind RNAPII (38) or the position of the arrest on the octamer surface (11,13). In either case, Spt4/5 acted on the nucleosomal intermediate that has DNA re-wrapped behind RNAPII. The reason why Spt4/5 had no effect on transcription through the 601 nucleosome is that DNA remains unwrapped behind RNAPII (11): the intermediate that Spt4/5 acts on never forms and the requirement for Spt4/5 is relieved.

Since Spt4/5 protects a few base pairs of DNA emerging from RNAPII (24,25,27,48), a conceptually attractive

model for how Spt4/5 promotes transcription through the nucleosome is that it regulates DNA re-wrapping behind RNAPII. A possibility is that delaying or preventing re-wrapping of DNA behind polymerase prevents it from being trapped in the loop, allows RNAPII to capitalize on fluctuations in DNA–octamer interactions ahead of RNAPII, suppresses arrest at +50 and leads to the deeper penetration of RNAPII into the nucleosome (Figure 7A). The end product is the stabilization of a partially wrapped nucleosome stabilized by Spt4/5 (Figure 7A). Spt4/5 produces a novel arrest at +90 on the 601R sequence. It is likely that the requirement or strength of the effects of Spt4/5 on nucleosome transcription will be nucleosome specific throughout the genome, dependent upon the flexibility and strength of DNA–histone contacts within the nucleosome. It may be less important on permissive sequences than those capable of forming structures that trap RNAPII on the surface of the octamer. This possibility is worth testing on a genome-wide scale, but doing so is well beyond the scope of this work.

Consequences of Spt4/5 on the nucleosome

The increased lifetime of a partially unwrapped nucleosome during transcription and the repositioning of RNAPII on another 'face' of the octamer would present an accessible target for co-transcriptional histone modifying enzymes (Figure 6B). For example, the footprint of RNAPII arrested at +50 (and its backtracked location) would restrict the accessibility of the H2A repression domain (HAR). The HAR is buried by the DNA when the nucleosome is fully wrapped onto the surface of the octamer and is required for H2B ubiquitylation (49). Spt4/5-induced transition of RNAPII from the mid-point to the +90 site and stabilization of a partially wrapped state would make the HAR more accessible to the ubiquitylation machinery. The HAR domain is in close proximity to the FRET pair used in this study, and potentially accessible in a partially wrapped nucleosome. Alternatively, the nucleosome intermediates generated by Spt4/5 may be better substrates of Chd1, which has genetic ties to Spt5 (50,51). It is widely accepted that the transcription of the nucleosome is required for, or at least coupled to, the activity of chromatin remodeling factors. The ability of Spt4/5 to control histone–DNA interactions could make nucleosomes better substrates for remodeling activities. It was recently discovered that the CTR of Spt5 recruits Paf1c to elongation complexes to control co-transcriptional histone modifications and depleting or mutating Spt5 reduces histone H2B ubiquitylation (27,43–46,52). An attractive model is one where the 'core' of Spt4/5 stabilizes a RNAPII-nucleosome intermediate that can be acted upon by chromatin modifying factors tethered to the CTR through the Paf1c complex (Figure 6B). This provides the opportunity for Spt4/5 to coordinate the movement of RNAPII through the nucleosome with the modification of histones during elongation. This elegant mechanism is similar to how the C-terminal region of the large subunit of RNAPII delivers RNA processing factors to the transcript, and may represent a common strategy used by cells to coordinate the mechanical movement of molecular machines and enzymatic modifications to substrates generated by the process.

SUPPLEMENTARY DATA

Supplementary Data are available at NAR Online.

ACKNOWLEDGEMENTS

We thank Jianhua Fu of the Medical College of Wisconsin for RNAPII used in the initial stages of the studies and Song Tan and Dave Gilmour for providing plasmids. The members of the Center for Eukaryotic Gene Regulation are recognized for their feedback and comments during this study.

FUNDING

National Institutes of Health (NIH) [GM58672 to J.C.R., GM097286 to T-H. L.]. Funding for open access charge: NIH [GM58672].
Conflict of interest statement. None declared.

References

1. Luger,K., Mader,A.W., Richmond,R.K., Sargent,D.F. and Richmond,T.J. (1997) Crystal structure of the nucleosome core particle at 2.8[thinsp]A resolution. *Nature*, **389**, 251–260.
2. White,C.L., Suto,R.K. and Luger,K. (2001) Structure of the yeast nucleosome core particle reveals fundamental changes in internucleosome interactions. *EMBO J.*, **20**, 5207–5218.
3. Bintu,L., Ishibashi,T., Dangkulwanich,M., Wu,Y.-Y., Lubkowska,L., Kashlev,M. and Bustamante,C. (2012) Nucleosomal elements that control the topography of the barrier to transcription. *Cell*, **151**, 738–749.
4. Hodges,C., Bintu,L., Lubkowska,L., Kashlev,M. and Bustamante,C. (2009) Nucleosomal fluctuations govern the transcription dynamics of RNA polymerase II. *Science*, **325**, 626–628.
5. Kireeva,M.L., Hancock,B., Cremona,G.H., Walter,W., Studitsky,V.M. and Kashlev,M. (2005) Nature of the nucleosomal barrier to RNA polymerase II. *Mol. Cell*, **18**, 97–108.
6. Hsieh,F.K., Fisher,M., Újvári,A., Studitsky,V.M. and Luse,D.S. (2010) Histone Sin mutations promote nucleosome traversal and histone displacement by RNA polymerase II. *EMBO Rep.*, **11**, 705–710.
7. Kulaeva,O.I., Gaykalova,D.A., Pestov,N.A., Golovastov,V.V., Vassylyev,D.G., Artsimovitch,I. and Studitsky,V.M. (2009) Mechanism of chromatin remodeling and recovery during passage of RNA polymerase II. *Nat. Struct. Mol. Biol.*, **16**, 1272–1278.
8. Bondarenko,V.A., Steele,L.M., Újvári,A., Gaykalova,D.A., Kulaeva,O.I., Polikanov,Y.S., Luse,D.S. and Studitsky,V.M. (2006) Nucleosomes can form a polar barrier to transcript elongation by RNA polymerase II. *Mol. Cell*, **24**, 469–479.
9. Dangkulwanich,M., Ishibashi,T., Liu,S., Kireeva,M.L., Lubkowska,L., Kashlev,M. and Bustamante,C.J. (2013) Complete dissection of transcription elongation reveals slow translocation of RNA polymerase II in a linear ratchet mechanism. *Elife*, **2**, e00971.
10. Churchman,L.S. and Weissman,J.S. (2011) Nascent transcript sequencing visualizes transcription at nucleotide resolution. *Nature*, **469**, 368–373.
11. Gaykalova,D.A., Kulaeva,O.I., Volokh,O., Shaytan,A.K., Hsieh,F.-K., Kirpichnikov,M.P., Sokolova,O.S. and Studitsky,V.M. (2015) Structural analysis of nucleosomal barrier to transcription. *Proc. Natl. Acad. Sci. U.S.A.*, **112**, E5787–E5795.
12. Bintu,L., Kopaczynska,M., Hodges,C., Lubkowska,L., Kashlev,M. and Bustamante,C. (2011) The elongation rate of RNA polymerase determines the fate of transcribed nucleosomes. *Nat. Struct. Mol. Biol.*, **18**, 1394–1399.
13. Kulaeva,O.I., Hsieh,F.-K., Chang,H.-W., Luse,D.S. and Studitsky,V.M. (2013) Mechanism of transcription through a

nucleosome by RNA polymerase II. *Biochim. Biophys. Acta*, **1829**, 76–83.
14. Hsieh,F.-K., Kulaeva,O.I., Patel,S.S., Dyer,P.N., Luger,K., Reinberg,D. and Studitsky,V.M. (2013) Histone chaperone FACT action during transcription through chromatin by RNA polymerase II. *Proc. Natl. Acad. Sci. U.S.A.*, **110**, 7654–7659.
15. Belotserkovskaya,R., Oh,S., Bondarenko,V.A., Orphanides,G., Studitsky,V.M. and Reinberg,D. (2003) FACT facilitates transcription-dependent nucleosome alteration. *Science*, **301**, 1090–1093.
16. Luse,D.S., Spangler,L.C. and Újvári,A. (2011) Efficient and rapid nucleosome traversal by RNA polymerase II depends on a combination of transcript elongation factors. *J. Biol. Chem.*, **286**, 6040–6048.
17. Orphanides,G., Wu,W.-H., Lane,W.S., Hampsey,M. and Reinberg,D. (1999) The chromatin-specific transcription elongation factor FACT comprises human SPT16 and SSRP1 proteins. *Nature*, **400**, 284–288.
18. Orphanides,G., LeRoy,G., Chang,C.-H., Luse,D.S. and Reinberg,D. FACT, a factor that facilitates transcript elongation through nucleosomes. *Cell*, **92**, 105–116.
19. Kim,J., Guermah,M. and Roeder,R.G. (2010) The Human PAF1 complex acts in chromatin transcription elongation both independently and cooperatively with SII/TFIIS. *Cell*, **140**, 491–503.
20. Schweikhard,V., Meng,C., Murakami,K., Kaplan,C.D., Kornberg,R.D. and Block,S.M. (2014) Transcription factors TFIIF and TFIIS promote transcript elongation by RNA polymerase II by synergistic and independent mechanisms. *Proc. Natl. Acad. Sci. U.S.A.*, **111**, 6642–6647.
21. Ishibashi,T., Dangkulwanich,M., Coello,Y., Lionberger,T.A., Lubkowska,L., Ponticelli,A.S., Kashlev,M. and Bustamante,C. (2014) Transcription factors IIS and IIF enhance transcription efficiency by differentially modifying RNA polymerase pausing dynamics. *Proc. Natl. Acad. Sci. U.S.A.*, **111**, 3419–3424.
22. Xin,H., Takahata,S., Blanksma,M., McCullough,L., Stillman,D.J. and Formosa,T. (2009) yFACT induces global accessibility of nucleosomal DNA without H2A-H2B displacement. *Mol. Cell*, **35**, 365–376.
23. Tsunaka,Y., Fujiwara,Y., Oyama,T., Hirose,S. and Morikawa,K. (2016) Integrated molecular mechanism directing nucleosome reorganization by human FACT. *Genes Dev.*, **30**, 673–686.
24. Bernecky,C., Herzog,F., Baumeister,W., Plitzko,J.M. and Cramer,P. (2016) Structure of transcribing mammalian RNA polymerase II. *Nature*, **529**, 551–554.
25. Martinez-Rucobo,F.W., Sainsbury,S., Cheung,A.C.M. and Cramer,P. (2011) Architecture of the RNA polymerase–Spt4/5 complex and basis of universal transcription processivity. *EMBO J.*, **30**, 1302–1310.
26. Mayer,A., Lidschreiber,M., Siebert,M., Leike,K., Soding,J. and Cramer,P. (2010) Uniform transitions of the general RNA polymerase II transcription complex. *Nat. Struct. Mol. Biol.*, **17**, 1272–1278.
27. Crickard,J.B., Fu,J. and Reese,J.C. (2016) Biochemical analysis of yeast suppressor of Ty 4/5 (Spt4/5) reveals the importance of nucleic acid interactions in the prevention of RNA polymerase II arrest. *J. Biol. Chem.*, **291**, 9853–9870.
28. Thåström,A., Lowary,P.T., Widlund,H.R., Cao,H., Kubista,M. and Widom,J. (1999) Sequence motifs and free energies of selected natural and non-natural nucleosome positioning DNA sequences1. *J. Mol. Biol.*, **288**, 213–229.
29. Kruk,J.A., Dutta,A., Fu,J., Gilmour,D.S. and Reese,J.C. (2011) The multifunctional Ccr4–Not complex directly promotes transcription elongation. *Genes Dev.*, **25**, 581–593.
30. Zhang,Z., Wu,C.-H. and Gilmour,D.S. (2004) Analysis of polymerase ii elongation complexes by native gel electrophoresis: Evidence for a novel carboxyl-terminal domain-mediated termination mechanism. *J. Biol. Chem.*, **279**, 23223–23228.
31. Dutta,A., Babbarwal,V., Fu,J., Brunke-Reese,D., Libert,D.M., Willis,J. and Reese,J.C. (2015) Ccr4-Not and TFIIS function cooperatively to rescue arrested RNA polymerase II. *Mol. Cell. Biol.*, **35**, 1915–1925.
32. Babbarwal,V., Fu,J. and Reese,J.C. (2014) The Rpb4/7 module of RNA polymerase II is required for carbon catabolite repressor protein 4-negative on TATA (Ccr4-Not) complex to promote elongation. *J. Biol. Chem.*, **289**, 33125–33130.
33. Zheng,S., Crickard,J.B., Srikanth,A. and Reese,J.C. (2014) A Highly conserved region within H2B is important for fact to act on nucleosomes. *Mol. Cell. Biol.*, **34**, 303–314.
34. Saha,A., Wittmeyer,J. and Cairns,B.R. (2002) Chromatin remodeling by RSC involves ATP-dependent DNA translocation. *Genes Dev.*, **16**, 2120–2134.
35. Chang,H.W., Shaytan,A.K., Hsieh,F.K., Kulaeva,O.I., Kirpichnikov,M.P. and Studitsky,V.M. (2013) Structural analysis of the key intermediate formed during transcription through a nucleosome. *Trends Cell Mol. Biol.*, **8**, 13–23.
36. Lee,T.-H. (2009) Extracting kinetics information from single-molecule fluorescence resonance energy transfer data using hidden markov models. *J. Phys. Chem. B*, **113**, 11535–11542.
37. Zhang,Z., Fu,J. and Gilmour,D.S. (2005) CTD-dependent dismantling of the RNA polymerase II elongation complex by the pre-mRNA 3′-end processing factor, Pcf11. *Genes Dev.*, **19**, 1572–1580.
38. Ngo,T.T.M., Zhang,Q., Zhou,R., Yodh,J.G. and Ha,T. (2015) Asymmetric unwrapping of nucleosomes under tension directed by DNA local flexibility. *Cell*, **160**, 1135–1144.
39. Carey,M., Li,B. and Workman,J.L. (2006) RSC exploits histone acetylation to abrogate the nucleosomal block to RNA polymerase ii elongation. *Mol. Cell*, **24**, 481–487.
40. Újvári,A., Hsieh,F.-K., Luse,S.W., Studitsky,V.M. and Luse,D.S. (2008) Histone N-terminal tails interfere with nucleosome traversal by rna polymerase II. *J. Biol. Chem.*, **283**, 32236–32243.
41. Buning,R., Kropff,W., Martens,K. and van Noort,J. (2015) spFRET reveals changes in nucleosome breathing by neighboring nucleosomes. *J. Phys. Condens Matter*, **27**, 064103.
42. Saha,A., Wittmeyer,J. and Cairns,B.R. (2005) Chromatin remodeling through directional DNA translocation from an internal nucleosomal site. *Nat. Struct. Mol. Biol.*, **12**, 747–755.
43. Wier,A.D., Mayekar,M.K., Héroux,A., Arndt,K.M. and VanDemark,A.P. (2013) Structural basis for Spt5-mediated recruitment of the Paf1 complex to chromatin. *Proc. Natl. Acad. Sci. U.S.A.*, **110**, 17290–17295.
44. Mayekar,M.K., Gardner,R.G. and Arndt,K.M. (2013) The recruitment of the saccharomyces cerevisiae Paf1 complex to active genes requires a domain of Rtf1 That directly interacts with the Spt4-Spt5 complex. *Mol. Cell. Biol.*, **33**, 3259–3273.
45. Liu,Y., Warfield,L., Zhang,C., Luo,J., Allen,J., Lang,W.H., Ranish,J., Shokat,K.M. and Hahn,S. (2009) Phosphorylation of the transcription elongation factor Spt5 by yeast bur1 kinase stimulates recruitment of the PAF complex. *Mol. Cell. Biol.*, **29**, 4852–4863.
46. Qiu,H., Hu,C., Gaur,N.A. and Hinnebusch,A.G. (2012) Pol II CTD kinases Bur1 and Kin28 promote Spt5 CTR-independent recruitment of Paf1 complex. *EMBO J.*, **31**, 3494–3505.
47. Chua,E.Y., Vasudevan,D., Davey,G.E., Wu,B. and Davey,C.A. (2012) The mechanics behind DNA sequence-dependent properties of the nucleosome. *Nucleic Acids Res.*, **40**, 6338–6352.
48. Klein,B.J., Bose,D., Baker,K.J., Yusoff,Z.M., Zhang,X. and Murakami,K.S. (2011) RNA polymerase and transcription elongation factor Spt4/5 complex structure. *Proc. Natl. Acad. Sci. U.S.A.*, **108**, 546–550.
49. Zheng,S., Wyrick,J.J. and Reese,J.C. (2010) Novel trans-Tail regulation of H2B ubiquitylation and H3K4 methylation by the N terminus of histone H2A. *Mol. Cell. Biol.*, **30**, 3635–3645.
50. Quan,T.K. and Hartzog,G.A. (2010) Histone H3K4 and K36 Methylation, Chd1 and Rpd3S oppose the functions of Saccharomyces cerevisiae Spt4–Spt5 in transcription. *Genetics*, **184**, 321–334.
51. Simic,R., Lindstrom,D.L., Tran,H.G., Roinick,K.L., Costa,P.J., Johnson,A.D., Hartzog,G.A. and Arndt,K.M. (2003) Chromatin remodeling protein Chd1 interacts with transcription elongation factors and localizes to transcribed genes. *EMBO J.*, **22**, 1846–1856.
52. Krogan,N.J., Kim,M., Ahn,S.H., Zhong,G., Kobor,M.S., Cagney,G., Emili,A., Shilatifard,A., Buratowski,S. and Greenblatt,J.F. (2002) RNA polymerase II elongation factors of saccharomyces cerevisiae: a targeted proteomics approach. *Mol. Cell. Biol.*, **22**, 6979–6992.